Abdominal Imaging

Published online: 17 February 2015

Abdom Imaging (2015) 40:1500–1509
DOI: 10.1007/s00261-015-0380-5

Budd–Chiari syndrome: a prospective analysis of hepatic vein obstruction on ultrasonography, multidetector-row computed tomography and MR imaging

Sid Ahmed Faraoun,[1] Mohamed El Amine Boudjella,[2] Nabil Debzi,[3] Nawel Afredj,[3] Youcef Guerrache,[1] Naima Benidir,[4] Chafik Bouzid,[5] Kamel Bentabak,[5] Philippe Soyer,[6] Salah Eddine Bendib[7]

[1]Department of Radiology, Centre Pierre et Marie Curie, Place du 1er Mai, 16016 Alger, Algeria
[2]Department of Internal Medicine, Hôpital de Kouba, Alger, Algeria
[3]Department of Hepatology, CHU Mustapha, Place du 1er Mai, 16016 Alger, Algeria
[4]Department of Pathology, Hôpital de la SûretéNationale, Alger, Algeria
[5]Department of Surgery, Centre Pierre et Marie Curie, Place du 1er Mai, 16016 Alger, Algeria
[6]Department of Body & Interventional Imaging, Hôpital Lariboisière-APHP & Université Diderot-Paris 7, 2 rue Ambroise Paré, 75010 Paris, France
[7]Department of Radiology & Université Benyoucef Benkhedda d'Alger, Centre Pierre et Marie Curie, Place du 1er Mai, 16016 Alger, Algeria

Abstract

Purpose: The goal of this study was to prospectively describe the imaging presentation of hepatic vein (HV) obstruction in patients with Budd–Chiari syndrome (BCS) on duplex and color Doppler ultrasonography (DCD-US), multidetector-row computed tomography (MDCT) and magnetic resonance imaging (MRI).
Materials and methods: A total of 176 patients with primary BCS (mean age, 33 years; 101 women) were prospectively included. BCS diagnosis was made by direct visualization of HV and/or upper portion of the inferior vena cava (IVC) obstruction on DCD-US and/or MDCT and/or MRI. Location (right, middle, and left HV), type (thrombus, stenosis, or both), and age (recent vs. long-standing) of HV obstruction were described on each imaging examination.
Results: HV obstruction was a constant (100%) finding and associated with IVC abnormalities in 51/176 (28.98%) patients. Obstruction of the three HVs was present in 158/176 (89.77%) patients. The prevalences of right, middle, and left HV thrombus were 151/169 (89.35%), 146/169 (86.39%), and 111/169 (65.68%), respectively. Long-standing HV thrombus was observed in more than 92% of patients on the three imaging methods. Agreement between DCD-US, MDCT, and MRI was perfect in the identification of long-standing HV thrombus ($\kappa = 0.9$); this agreement was slight to moderate in revealing the type of HV abnormality (i.e., fibrotic cord and non-visible HV).
Conclusion: Our results indicate that BCS is a chronic and insidious disease, more often discovered at an advanced stage. These results should warrant further evaluation of screening strategies in patients with risk factors for BCS to identify the disease at an early stage.

Key words: Budd–Chiari syndrome—Hepatic vein—Thrombosis—Imaging

Abbreviations

BCS	Budd–Chiari syndrome
HV	Hepatic vein
IVC	Inferior vena cava
DCD-US	Duplex color Doppler ultrasonography
MDCT	Computed tomography
MRI	Magnetic resonance imaging
TE	Echo time
TR	Repetition time

Correspondence to: Sid Ahmed Faraoun; *email:* faraounsid@yahoo.fr

TSE	Turbo spin echo
ms	Milliseconds
KV	Kilovolts
US	Ultrasonography
Ns	Not specified

Budd–Chiari Syndrome (BCS) is a serious condition, which is defined as a combination of clinical and biological manifestations resulting from impaired hepatic venous drainage, regardless the cause and location [1–4]. The causative lesion of BCS can be located on any portion of the hepatic venous drainage path, from the hepatica venula to upper portion of the inferior vena cava (IVC) [5]. This definition excludes drainage abnormalities of the hepatic venous system secondary to cardiac insufficiency, pericardium disease, and veino-occlusive disease of the liver [2].

BCS is commonly classified into primary or secondary BCS [6]. Primary BCS is the consequence of a venous obstruction that is due in most cases to thrombosis and less frequently to hepatic vein stenosis. Secondary BCS results from venous obstruction due to an external compression by a tumor or by an infectious process [4, 6–8]. The etiologies of primary BCS and location of causative lesions greatly vary among countries. In Europe, BCS is most commonly secondary to hepatic vein (HV) thrombosis, whereas in Asia and South Africa, BCS is mostly secondary to a diaphragmatic stenosis of the IVC, which corresponds to the fibrous or membranous transformation of a thrombus.

In clinical practice, imaging is the starting point of the investigation of patients with BCS to determine the type and location of the obstructive lesions. To date, a few published studies have described these various aspects of the disease [9–17] although differentiation between the different types of HV occlusion is of major importance because they require specific treatments that may greatly differ [10].

The goal of this study was to prospectively assess the presentation of HV obstruction on duplex and color Doppler ultrasonography (DCD-US), multidetector-row computed tomography (MDCT) and magnetic resonance imaging (MRI).

Materials and methods

Patients

From July 2008 to July 2012 inclusively, 176 consecutive patients presenting with primary BCS were prospectively included in the study. All patients were referred from the Department of Liver Diseases of our institution, which is the national reference center for BCS. They were 101 women and 75 men (sex ratio: 0.74), with a mean age of 33 years ± 11 (SD) (range: 12–70 years). Inclusion criteria were BCS with a primary obstruction of HV and/or upper portion of IVC. Exclusion criteria were BCS secondary to tumor, BCS secondary to infectious disease, and BCS associated with advanced or pre-existing cirrhosis. The average time between the onset of symptoms and imaging was 13 months (range: 1–120 months). An underlying thrombotic disease and/or one or more risk factors for venous thrombosis were present in 82/176 (46.59%) patients. Acquired predisposing factors for thrombophilia (mostly myeloproliferative syndromes) were present in 57/176 (32.39%) patients. Inherited causes of thrombophilia (Protein S deficiency, Protein C deficiency, or hyperhomocysteinemia) were present in 9/176 (5.11%) patients. Celiac disease was present in 12/176 (6.82%) patients. The study was approved by our Institutional Review Board and informed consent was obtained from all patients. The study was funded by a grant from the Ministry of Health. Imaging examinations were performed at no charge for the patients.

Diagnostic criteria of BCS

On imaging, the diagnosis of BCS was made by direct visualization of a thrombus in at least one main HV and/or a thrombus in the suprahepatic segment of the IVC, and/or HV stenosis on DCD-US, MDCT, or MRI.

BCS was classified clinically into three categories including acute, subacute, and chronic BCS [18]. The acute form was diagnosed in the presence of painful hepatomegaly, ascites, severe hepatocellular failure, and serum transaminase level $>5\times$ normal value. The chronic form was diagnosed in the presence of superficial thoraco-abdominal collateral venous circulation and/or symptomatic or asymptomatic clinical and biological chronic liver disease with moderate abnormalities of liver function tests. The subacute form was diagnosed in the presence of at least one criterion of the acute form associated with at least one criterion of the chronic form. This classification did not consider the time interval between onset of symptoms and imaging examination.

Imaging techniques

DCD-US. DCD-US was first performed in all patients once the diagnosis of BCS was suspected. DCD-US examinations were performed with a commercially available SSD-5000 sonographic unit (Hitachi Aloka Medical, Ltd., Tokyo, Japan) by two different radiologists with experience in ultrasonography. Ultrasonographic parameters (gain, filter, frequency, focus, and harmonic imaging) were adapted depending on the explored anatomic area. Color and pulsed Doppler image acquisition was optimized by adjusting insonation angle, wall filters, sample volume length, color priority, pulse repetition frequency, and ultrasound gain. The final velocity estimates, calculated with a window of sampling placed in the center of the vessel and covering two-thirds

of the vessel lumen, were recorded only for firing angles ≤40°. The portal vein and hepatic artery were analyzed using an oblique angle through an intercostal approach. This allowed obtaining a favorable firing angle for vessel analysis. The full DCD-US examination was performed in an average time of 20 min.

MDCT. MDCT examinations were performed with a 16-section MDCT unit (Sensation 16, Siemens Healthcare, Forchheim, Germany). Scanning parameters were as follows: collimation thickness, 1.5 mm; beam collimation, 24 mm; field of view, 280–450 mm; tube potential, 130 kV; tube current, 190 mAs; and beam pitch, 0.85. Axial MDCT images were reconstructed with a thickness of 2 mm.

A first set was obtained before intravenous administration of iodinated contrast material. All patients received iodinated contrast material (meglumine ioxitalamate, Telebrix 350®, Laboratoire Guerbet, Roissy-Charles de Gaulle, France) at a dose of 2 cc/kg of body weight with an automatic power injector, at a rate of 4 cm^3/s. A second data set covering the liver (arterial phase) and a third data set covering the entire abdomen, pelvis, and thorax (portal phase) were obtained at 30 and 70 s, respectively, after the start of contrast injection. A fourth data set covering the entire abdomen and pelvis (late phase) and a fifth data set covering the liver (delayed phase) were obtained at 2 and 3 min, respectively. The full MDCT examination, including patient preparation, was performed in an average time of 20 min.

Reconstructed images were obtained on a workstation equipped with the Syngo software (Leonardo, Siemens Healthcare) allowing various reconstruction modes.

MRI. MRI examinations were performed with a 1.5-T unit (Avanto, Siemens Healthcare, Forchheim, Germany) using a phased-array multicoil. Parallel imaging with generalized autocalibrating partially parallel acquisition (GRAPPA) was used with an acceleration factor (or reduction factor) of 2. All patients underwent T1-weighted spin echo sequence using an in-phase (TR/TE, 180/4.7 ms) and opposed-phase (TR/TE, 180/2.3 ms) imaging with 80° flip angle and 6-mm-thick axial sections. A breath-hold T2-weighted MR sequence was obtained in the axial and coronal planes using a HASTE sequence (TR/TE, 900/88 ms; 150° flip angle, 5-mm section thickness). In addition, heavily T2-weighted turbo spin echo (TSE) sequence (TR/TE, 3500/400 ms; inversion time, 68–80/165 ms; refocusing pulse, 130; bandwidth, 325 Hz/pixel; 6-mm section thickness) was performed in the axial plane.

Fat-suppressed three-dimensional low-angle volumetric interpolated breath-hold (3D VIBE) T1-weighted gradient echo MR sequence (TR = 3.8–5.2 ms; TE = 1.6–1.9 ms; flip angle, 12°; bandwidth, 488 Hz/pixel) was used for dynamic imaging. 3D VIBE sequences were obtained before and after intravenous administration of 0.2 mg/kg of gadoterate meglumine (Dotarem®, Guerbet, Roissy-Charles de Gaulle, France) at a rate of 3 mL/s followed by a 20 mL flush of normal saline via a power injector. Arterial phase 3D VIBE images were acquired with a real-time bolus-tracking method 8 s after the arrival of contrast material in the celiac trunk. Portal and further delayed 3D VIBE sequences were acquired 70, 120, and 180 s, respectively, after the beginning of contrast administration. The full MRI examination, including patient preparation, was performed in an average time of 25 min.

Image analysis

DCD-US, MDCT, and MRI were performed in all patients less than 12 days from each other. DCD-US, MDCT, and MRI examinations were interpreted prospectively by a panel of five radiologists using a standardized data collection form. Each examination involving an individual patient was interpreted by two radiologists working together who reached a consensus opinion, blinded to the results of the other two examinations. Each visible HV was categorized as right, middle, or left following the well-established description developed by Couinaud [19]. For each examination, the radiologist recorded the number of visible HVs (1, 2, or 3 HVs), the number and location (1, 2, or 3 HVs and right, middle, left HV) of abnormal HVs, the appearance of the intraluminal content of each HV, the presence of HV thrombus, and the presence of HV stenosis. HV stenoses were further categorized into short-length or long-length stenosis. Additional variables including non-visible HV and cord-like transformation were recorded depending on the specific imaging examination.

On DCD-US, the diagnosis of recent HV thrombus was made when the HV had hyperechogenic content in association with an absent venous outflow within the HV. On MDCT, the diagnosis of recent HV thrombus was made when no enhancement was present within the HV due to an obliterating thrombus that was spontaneously hypoattenuating on unenhanced MDCT images. On MR imaging, the diagnosis of recent HV thrombus was made when no enhancement after gadolinium chelate administration was present within the HV due to an obliterating thrombus. Persistence of HV lumen upstream and/or downstream to thrombus in case of focal thrombus and the absence of venous wall remodeling were the other two diagnostic criteria used for the diagnosis of recent thrombus whatever the imaging technique used.

The diagnosis of long-standing HV thrombus was made when DCD-US, MDCT, or MRI showed no venous flow due to fibrotic cord replacing a normal HV with a hyperechoic, hypoattenuating, or hypointense appearance, respectively. In addition, long-standing HV thrombus was considered when non-visible HV was associated with intrahepatic collateral vessels.

On DCD-US, HV stenosis was considered in the presence of aliasing or mosaic color indicating turbulence in the narrowed HV on color images. On pulsed Doppler analysis HV stenosis was considered in the presence persistent flow with an increased velocity (flow speed >1 m/s), flow demodulation upstream the narrowed area with a continuous, slow, or reversed blood flow. On MDCT and MRI, a stenosis was considered hemodynamically significant when findings indicating venous hypertension were present; they included HV dilation upstream to stenosis, late vascular enhancement, collateral circulation, or mosaic pattern of enhancement of hepatic parenchyma. HV stenosis was considered short if its length was <20 mm and long when the length was ≥ 20 mm. HV stenosis limited to the HV ostium or to the common left medial trunk, with an upstream patent HV segment was categorized as ostial.

Statistical analysis

Statistical analyses were performed using software (StatView 5.0, Abacus Concepts Inc, Palo Alto, CA, USA). Descriptive statistics were calculated for all variables evaluated at imaging. Qualitative (binary) data included raw numbers, proportions, and frequencies. The proportions of positive findings on the three imaging examinations were calculated with their 95% confidence intervals (CIs). Differences in proportions of imaging findings between the three imaging techniques were searched for using the Mc Nemar test. A P value of less than 0.05 was considered to indicate significance. The concordance between DCD-US, MDCT, and MRI was evaluated using the Kappa test.

Results

According to the diagnostic criteria as defined above, acute, subacute, and chronic clinical forms of BCS were found in 11/176 (6.25%), 29/176 (16.48%), and 136/176 (77.27%) patients, respectively. HV obstruction was observed in all patients (176/176; 100%) and in association with abnormalities of the upper portion of the IVC in 51/176 (28.98%) patients. No patients had abnormalities of the upper portion of the IVC only on any of the three imaging techniques.

Obstruction of the three HVs was noted in 157/176 (89.20%) patients on DCD-US and MRI and in 158/176 (89.77%) patients on MDCT. Obstruction of two HVs, which included the middle HV in all patients, was observed in 12/176 (6.82%) patients on DCD-US and MRI

Table 1. HV obstruction characteristics according to the number and location of HVs at imaging

Number of HVs	HV location	DCD-US *n* (%)	MDCT *n* (%)	MRI *n* (%)
3	Right + middle + left	157/176 (89.20) [83.66–93.77]	158/176 (89.77) [84.32–93.82]	157/176 (89.20) [83.66–93.77]
2	Right + middle	7/176 (3.98) [1.61–8.02]	6/176 (3.41) [1.26–7.37]	6/176 (3.41) [1.26–7.37]
	Middle + left	5/176 (2.84) [0.95–6.50]	5/176 (2.84) [0.95–6.50]	6/176 (3.41) [1.26–7.37]
1	Middle	4/176 (2.27) [0.62–5.72]	4/176 (2.27) [0.62–5.72]	4/176 (2.27) [0.62–5.72]
	Right	3/176 (1.70) [0.35–4.90]	3/176 (1.70) [0.35–4.90]	3/176 (1.70) [0.35–4.90]
	Left	0/176 (0) [0.00–2.07]	0/176 (0) [0.00–2.07]	0/176 (0) [0.00–2.07]

HV indicates hepatic vein. DCD-US indicates duplex and color Doppler ultrasonography. MDCT indicates multidetector-row computed tomography. MRI indicates magnetic resonance imaging. Numbers in brackets indicate 95% confidence intervals

Table 2. Distribution of the nature of HV obstruction in 176 patients

Nature of HV obstruction	DCD-US *n* (%)	MDCT *n* (%)	MRI *n* (%)
Thrombus	115/176 (65.34) [57.81–72.34]	122/176 (69.32) [61.94–76.04]	121/176 (68.75) [61.34–75.51]
Thrombus and stenosis	54/176 (30.68) [23.96–38.06]	48/176 (27.27) [20.84–34.48]	49/176 (27.84) [21.36–25.08]
Stenosis	7/176 (3.98) [1.61–8.02]	6/176 (3.41) [1.26–7.37]	6/176 (3.41) [1.26–7.37]
Total	176 (100%)	176 (100%)	176 (100)

HV indicates hepatic vein. DCD-US indicates duplex and color Doppler ultrasonography. MDCT indicates multidetector-row computed tomography. MRI indicates magnetic resonance imaging. Numbers in brackets indicate 95% confidence intervals

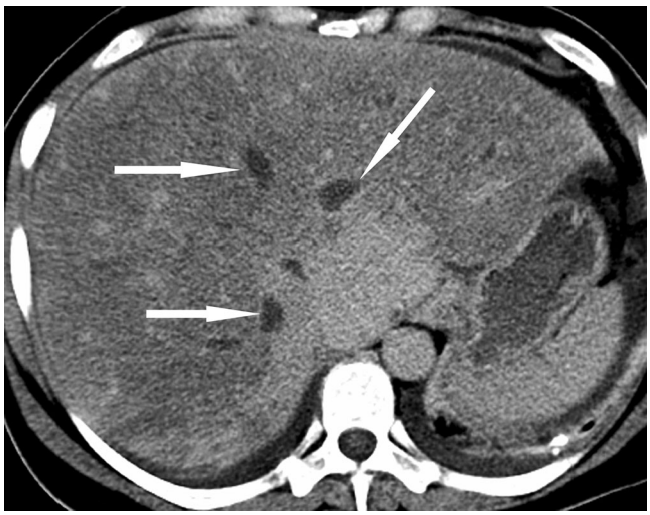

Fig. 1. 28-year-old man with protein S deficiency who developed acute BCS. MDCT image in the axial plane obtained after intravenous administration of iodinated contrast material during the portal phase shows hypoattenuating thrombus involving right, middle, and left hepatic veins (*arrows*).

and in 11/176 (6.25%) patients on MDCT. Obstruction of the left HV alone was never observed on any of the three imaging techniques (Table 1). No differences in imaging presentation were observed between the patients with BCS due to myeloproliferative syndrome and those with BCS due to another condition.

HV thrombus

HV thrombus was observed in 169/176 (96.02%) patients on DCD-US and 170/176 (96.59%) patients on MDCT and MRI (Table 2). HV thrombus was associated with HV stenosis in 54/176 (30.68%) patients on DCD-US, 48/176 (27.27%) on MDCT, and 49/176 (27.84%) on MRI.

On DCD-US, among the 169 patients in whom HV thrombus was observed, the thrombus involved the right, middle, and left HV in 151/169 (89.35%), 146/169 (86.39%), and 111/169 (65.68%) patients, respectively. On MDCT and MRI, thrombus in the right, middle, and left HV was observed in 151/170 (88.82%), 151/170 (85.79%), and 118/170 (69.41%) patients, respectively (Fig. 1).

Thrombus in three HVs or two HVs was more frequently observed than thrombus in a single HV, which was seen in 21/169 (12%) patients. Thrombus in the left HV alone was never observed on any of the three imaging techniques (Table 3).

Thrombus involved the whole HV lumen in 160/169 (94.67%) patients on DCD-US and in 161/170 (94.71%) patients on MDCT and MRI. Thrombus involved the ostium of a single HV in 9/169 (5.33%) patients on DCD-US and in 9/170 (5.29%) on MDCT and MRI.

Long-standing HV thrombus was observed in the majority of patients. This type of abnormality was seen on DCD-US, on MDCT, and on MRI in 156/169 (92.31%), 157/170 (92.35%), and 157/170 (92.35%) patients, respectively, with no significant differences between the three techniques (Mc Nemar test, $P = 0.1$). Recent thrombus involving three HVs with no collateral circulation was observed in 7/171 (4%). An association between recent and long-standing HV thrombus was observed in 15/169 (8.88%) patients on DCD-US, 14/170 (8.24%) patients on MDCT, and 13/170 (7.65%) patients on MRI.

A fibrotic cord replacing a normal HV was visible in 106/169 (62.72%) patients on DCD-US, 36/170 (21.30%) patients on MDCT, and 44/170 (25.88%) patients on MRI (Figs. 2, 3, 4). Significant differences were found between DCD-US and the other two imaging techniques ($P < 0.001$), and between MDCT and MRI

Table 3. HV thrombus characteristics according to the number and location of HVs at imaging

Number of HVs	Type of HV	US *n* (%)	MDC *n* (%)	MRI *n* (%)
3	Right + middle + left	96/169 (56.80) [48.98–64.39]	104/170 (61.18) [53.41–68.54]	103/170 (60.58) [52.82–67.98]
2	Right + middle	32/169 (18.93) [13.33–25.67]	28/170 (16.47) [11.23–22.92]	28/170 (16.47) [11.23–22.92]
	Middle + left	13/169 (7.69) [4.16–12.79]	13/170 (7.65) [4.13–12.72]	13/170 (7.65) [4.13–12.72]
	Right + left	2/169 (1.18) [0.14–4.21]	1/170 (0.59) [0.01–3.23]	2/170 (1.18) [0.14–4.19]
1	Right	21/169 (12.43) [7.86–18.37]	18/170 (10.59) [6.40–16.22]	18/170 (10.59) [6.40–16.22]
	Middle	5/169 (2.96) [0.97–6.67]	6/170 (3.53) [1.31–7.52]	6/170 (3.53) [1.31–7.52]
	Left	0/169 (0) [0–2.16]	0/170 (0) [0–2.15]	0/170 (0) [0–2.15]

HV indicates hepatic vein. DCD-US indicates duplex and color Doppler ultrasonography. MDCT indicates multidetector-row computed tomography. MRI indicates magnetic resonance imaging. Denominators vary because the number of visible HV varied depending on the imaging technique. Numbers in brackets indicate 95% confidence intervals

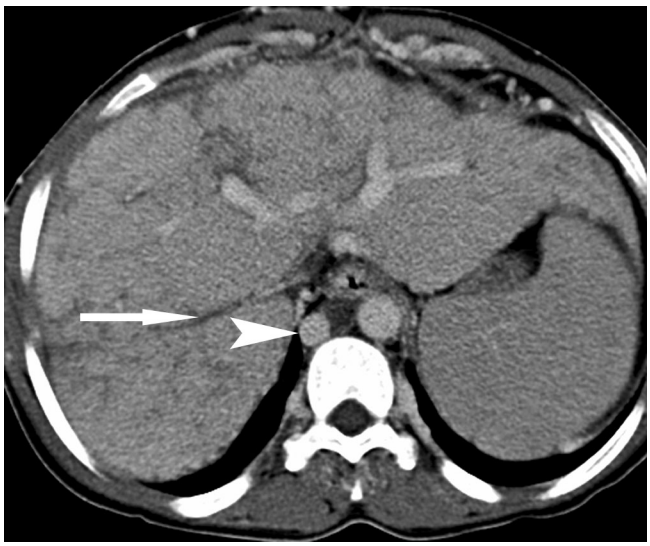

Fig. 2. 25-year-old woman with celiac disease who developed chronic BCS. MDCT image in the axial plane obtained during the portal phase shows hypoattenuating fibrous cord (*arrow*) replacing the right hepatic vein. Dilated azygos vein (*arrowhead*) is also seen, representing vertebrolumbar venous collateral pathways.

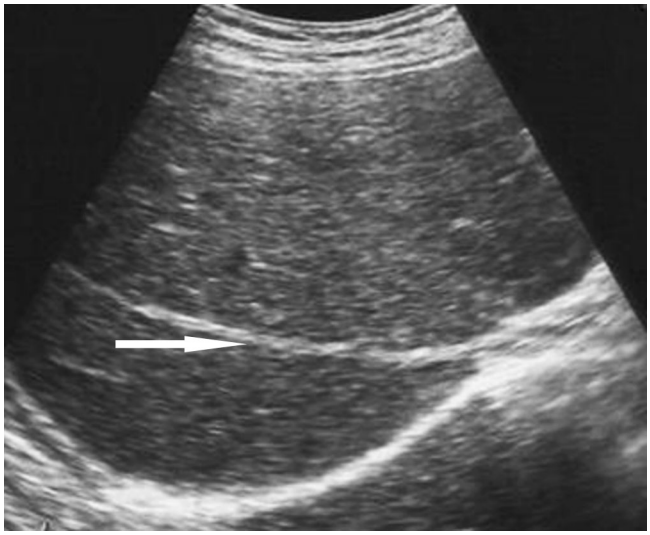

Fig. 3. 38-year-old man with myeloproliferative disease who developed chronic BCS. T2-weighted MR image obtained using the HASTE sequence in the coronal plane shows hypointense fibrous cord (*arrow*) replacing the right hepatic vein. Heterogeneous hepatomegaly is also present.

($P = 0.0133$) for the presence of fibrotic cords. Non-visible HV was noticed in 13/169 (7.69%) patients on DCD-US, 72/170 (42.35%) patients on MDCT, and 58/170 (34.12%) patients on MRI (Fig. 5). Similarly, significant differences between the three imaging techniques were found for the presence of non-visible HV ($P < 0.001$). Association between fibrotic cord replacing a normal HV and non-visible HV was noticed in 32/169

Fig. 4. 40-year-old woman with an 8-month history of weakness and jaundice. Ultrasonography shows hyperechogenic fibrous cords (*arrow*) replacing the right hepatic vein. These findings are consistent with chronic BCS.

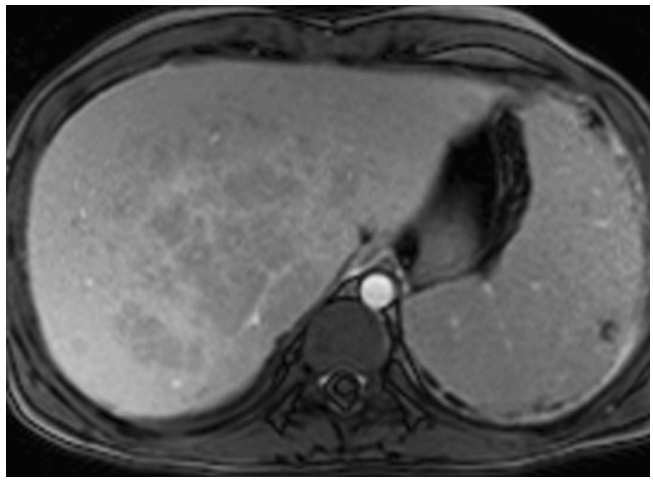

Fig. 5. 42-year-old man with myeloproliferative disease who developed chronic BCS. On fat-suppressed T1-weighted MR image in the axial plane obtained during the portal venous phase after intravenous administration of a gadolinium chelate, the three HVs are not visible. In addition, MR image shows heterogeneous enhancement of hepatic parenchyma, splenomegaly, and extrinsic compression of the inferior vena cava, which is not visible.

(18.93%) patients on DCD-US, 43/170 (25.29%) patients on MDCT, and 49/170 (28.82%) patients on MRI.

Isolated long-standing HV thrombus was present in all patients (130/130; 100%) with chronic BCS and in 11/

Table 4. Distribution of the nature of HV obstruction on a vein-by-vein analysis

	DCD-US *n* (%)	MDCT *n* (%)	MRI *n* (%)
Right HV			
Non-visible	16/176 (9.09) [5.29–29.34]	69/176 (39.20) [31.95–46.83]	60/176 (34.09) [27.13–41.60]
Thrombus	11/176 (6.25) [3.16–10.91]	11/176 (6.25) [3.16–10.91]	11/176 (6.25) [3.16–10.91]
Short-length stenosis	5/176 (2.84) [0.93–6.50]	5/176 (2.84) [0.93–6.50]	5/176 (2.84) [0.93–6.50]
Long-length stenosis	11/176 (6.25) [3.16–10.91]	11/176 (6.25) [3.16–10.91]	11/176 (6.25) [3.16–10.91]
Cord-like transformation	124/176 (70.45) [63.12–77.08]	71/176 (40.34) [33.03–47.99]	80/176 (45.45) [37.95–53.12]
Normal	9/176 (5.11) [2.36–9.49]	9/176 (5.11) [2.36–9.49]	9/176 (5.11) [2.36–9.49]
Middle HV			
Non-visible	26/176 (14.77) [9.88–20.89]	73/176 (41.48) [34.11–49.13]	63/176 (35.80) [28.72–43.36]
Thrombus	20/176 (11.36) [7.08–17]	20/176 (11.36) [7.08–17]	20/176 (11.36) [7.08–17]
Short-length stenosis	20/176 (11.36) [7.08–17]	17/176 (9.66) [5.73–15.01]	17/176 (9.66) [5.73–15.01]
Long-length stenosis	10/176 (5.68) [2.76–10.20]	5/176 (2.84) [0.93–6.50]	6/176 (3.41) [1.26–7.27]
Cord-like transformation	100/176 (56.82) [49.15–64.25]	58/176 (32.95) [26.07–40.43]	67/176 (38.07) [30.87–45.68]
Normal	3/176 (1.70) [0.35–4.90]	3/176 (1.70) [0.35–4.90]	3/176 (1.70) [0.35–4.90]
Left HV			
Non-visible	22/176 (12.50) [8.00–18.31]	68/176 (38.64) [31.41–46.26]	59/176 (33.52) [26.60–41.01]
Thrombus	11/176 (6.25) [3.16–10.91]	11/176 (6.25) [3.16–10.91]	11/176 (6.25) [3.16–10.91]
Short-length stenosis	40/176 (22.73) [16.76–29.64]	40/176 (22.73) [16.76–29.64]	40/176 (22.73) [16.76–29.64]
Long-length stenosis	11/176 (6.25) [3.16–10.91]	5/176 (2.84) [0.93–6.50]	5/176 (2.84) [0.93–6.50]
Cord-like transformation	78/176 (44.32) [36.85–51.98]	38/176 (21.59) [15.76–28.41]	47/176 (26.70) [20.33–33.88]
Normal	14/176 (7.95) [4.42–12.99]	14/176 (7.95) [4.42–12.99]	14/176 (7.95) [4.42–12.99]

HV indicates hepatic vein. DCD-US indicates duplex and color Doppler ultrasonography. MDCT indicates multidetector-row computed tomography. MRI indicates magnetic resonance imaging. Numbers in brackets indicate 95% confidence intervals

29 (37.93%) patients with subacute BCS. Isolated recent HV thrombus was observed in all patients (11/11; 100%) with acute BCS, in 2/29 (6.90%) patients with subacute BCS, and in no patients with chronic BCS. Association between recent and long-standing HV thrombus was exclusively observed in patients with subacute BCS, with a prevalence of 55.17% (16/29).

An almost perfect agreement ($\kappa = 0.9$) was found between DCD-US, MDCT, and MRI in the identification of long-standing HV thrombus. Agreement was slight to moderate in revealing the type of HV abnormality. Indeed, kappa values for agreement between DCD-US and MRI, DCD-US and MDCT were, respectively, 0.19 and 0.17 for the fibrotic cords. They were 0.56 and 0.25 for non-visible HV.

The prevalences of HV thrombus, fibrotic cords, non-visible HV, HV stenosis, and normal HV among the 528 HVs analyzed were 42/528 (7.95%), 302/528 (57.19%), 64/528 (12.12%), 94/528 (17.80%), and 26/528 (4.92%) on DCD-US, respectively. They were 42/528 (7.95%), 167/528 (13.62%), 210/528 (39.77%), 83/528 (15.71%), and 26/528 (4.92%) on MDCT, respectively. They were 42/528 (7.95%), 194/528 (36.74%), 182/528 (34.46%), 84/528 (15.90%), and 26/528 (4.92%) on MRI, respectively. Indeed, 160/167 HV fibrotic cords present on MCDT and 187/194 HV fibrotic cords present on MRI corresponded to fibrotic cords on DCD-US. Conversely, 98/210 non-visible HVs on MDCT and 83/182 non-visible HVs on MRI corresponded to fibrotic cords on DCD-US (Table 4).

HV stenosis

HV stenosis was observed in 61/176 (34.66%) patients on DCD-US, 54/176 (30.68%) patients on MDCT, and 55/176 (31.25%) patients on MRI. Significant differences were found between DCD-US and MDCT ($P = 0.0233$) and between DCD-US and MRI ($P = 0.0412$), but not

Table 5. HV stenosis characteristics according to the number and location of HVs on imaging

Number of HVs	Type of HV	DCD-US *n* (%)	MDCT *n* (%)	MRI *n* (%)
3	Right + middle + left	7/61 (11.48) [4.74–22.20]	6/54 (11.11) [4.19–22.6]	6/55 (10.91) [4.11–22.25]
2	Middle + left	18/61 (29.51) [1.52–42.57]	15/54 (27.78) [16.46–41.64]	15/55 (27.27) [16.14–40.96]
	Right + left	1/61 (1.64) [0.04–8.80]	2/54 (3.70) [0.40–12.70]	2/55 (3.64) [0.40–12.53]
1	Left	25/61 (40.98) [28.55–54.32]	22/54 (40.74) [27.57–54.97]	22/55 (40) [27.02–54.09]
	Right	8/61 (13.11) [5.80–24.20]	8/54 (14.81) [6.62–27.12]	8/55 (14.55) [6.50–26.66]
	Middle	2/61 (3.28) [0.40–11.35]	1/54 (1.86) [0.05–9.89]	2/55 (3.64) [0.40–12.53]

HV indicates hepatic vein. DCD-US indicates duplex and color Doppler ultrasonography. MDCT indicates multidetector-row computed tomography. MRI indicates magnetic resonance imaging. Denominators vary because the number of visible HV varied depending on the imaging technique. Numbers in brackets indicate 95% confidence intervals

between MDCT and MRI ($P > 0.999$) for the presence of HV stenosis. HV stenosis alone in the absence of associated HV thrombus was observed in 7/176 (3.98%) patients on DCD-US and 6/176 (3.41%) patients on MDCT and MRI with no statistically significant difference ($P > 0.999$).

Stenosis of a single HV was observed in 35/61 (57.38%) patients on DCD-US, 31/54 (57.41%) patients on MDCT, and 32/55 (58.18%) patients on MRI and predominantly involved the left HV (Table 5). Stenosis of two HVs was observed in 19/61 (31.15%) patients on DCD-US, 17/54 (31.48%) patients on MDCT, and 17/55 (30.91%) patients on MRI. Stenosis of the main three HVs was seen in 7/61 (11.48%) patients on DCD-US, 6/54 (11.11%) patients on MDCT, and 6/55 (10.91%) patients on MRI.

When present, HV stenosis was located at the ostium of the HV in all patients and was found in association with non-ostial stenosis in 9/61 (14.75%) patients on DCD-US, 10/54 (18.52%) patients on MDCT, and 11/55 (20%) patients on MRI (Fig. 6).

Short HV stenosis was noted in 50/61 (81.97%) patients on DCD-US, 41/54 (75.93) patients on MDCT, and 42/55 (76.36%) patients on MRI with statistically significant differences between DCD-US and MDCT ($P = 0.008$) and MRI ($P = 0.013$), but not between MDCT and MRI ($P > 0.999$). Venous flow upstream to HV stenosis was monophasic in all patients with a reduced or reversed flow in 34/61 (55.74%) patients and 27/61 (44.26%) patients, respectively.

The kappa coefficient showed an almost perfect agreement ($\kappa = 0.9$) between DCD-US, MDCT, and MRI in the identification of HV stenosis.

Fig. 6. 32-year-old woman with thrombocythemia who developed chronic BCS. Maximum intensity projection (MIP) reformatted MDCT image in oblique plane obtained during the portal phase shows short ostial stenosis (*arrow*) of right hepatic vein.

Discussion

Our study describes the imaging findings in 176 patients with BCS due to HV obstruction. Of them, approximately one-third had an associated obstruction of the IVC. This presentation, which uniformly involves HV obstruction, is the most common one in Europe. In one series, the prevalence of HV involvement only, IVC involvement only, and the combination of both were 62%, 7%, and 31%, respectively [20]. A similar distribution was also noted in another European series [10], in which HV obstruction was constant and associated with IVC abnormalities in 20.9% of patients, while there was no isolated IVC obstruction. The results of our study are similar to those observed in European series [10, 20]. One reason may be that risk factors are similar.

In our study, no patients had BCS due to a diaphragm that totally or partially obstructs the upper portion of the IVC. The etiopathogenesis of diaphragmatic stenosis of the IVC is not fully elucidated yet, whereas its frequency varies among countries. It is at least 5 times more frequent in Asia than in Europe [9, 21]. In Nepal, this cause is virtually the single cause of BCS [22]. In China, IVC obstruction is present in 62% of patients with BCS [23]. This variant of BCS is exceptional in Europe, or even absent [3, 24].

In our study, we have prospectively collected the imaging findings observed on DCD-US, MDCT, and MRI with respect to the status of the HVs in patients with BCS. The presentation of HV thrombus varies according to its age and the imaging technique used. On DCD-US, the presence of echogenic material in the HV lumen indicates acute thrombus, which shows no signal on color Doppler ultrasonography. On MDCT and MRI, recent HV thrombus is more readily visible than the long-standing one. It presents with an hypoattenuating HV content on MDCT and a hypointense one on T1-weighted MR images, and is responsible for absent HV opacification after intravenous administration of contrast material. In case of long-standing thrombus, HV may present as a fibrotic cord, which is more visible on DCD-US, or may be not visible.

The prevalence of recent HV thrombus in BCS varies among series, ranging from 18% to 50% [17, 25]. Long-standing HV thrombus is far more common than recent HV thrombus, representing 75% of all cases of BCS in one study [17]. In a German study, long-standing HV thrombus was more frequently observed than recent HV thrombus; the prevalence of right, middle, and left HV thrombus was 64%, 57%, and 33%, respectively [11]. In the same study, a fibrotic cord was more frequently reported than non-visibility for the right HV (40% vs. 24%, respectively) and for the middle HV (33% vs. 24%, respectively), whereas non-visibility of HV was more frequently found than fibrotic cord for the left HV (13% vs. 20%, respectively [11].

In our study, long-standing HV thrombus was observed in 92.3% of patients. Furthermore, the frequencies with which the different patterns were observed depended on the specific imaging technique. In fact, fibrotic cords were more frequently observed on DCD-US (62.72%) than on MDCT (21.30%) or MRI (25.88%). By contrast, non-visible HVs were more frequently reported on MRI (34.12%) and MDCT (42.35%) than on DCD-US (7.69%). On the other hand, we found kappa value indicating almost perfect agreement ($\kappa = 0.9$) between DCD-US, MDCT, and MRI in the identification of long-standing HV thrombus. Conversely, kappa value was very low for non-visible HV with MRI and MDCT. Our results suggest that the three imaging techniques are equivalent and concordant for the diagnosis of long-standing HV thrombus. However, DCD-US offers the advantage of a better characterization of these HV abnormalities.

A few studies have analyzed the morphologic characteristics of HV stenosis. Boozari et al., using DCD-US, found ostial stenosis of the right, middle, and left HV in 6.7%, 4.4%, and 4.4% of patients, respectively [11]. In another study, HV stenosis of right, middle, or left HV was observed in 48%, 96%, and 96% of patients, respectively [10]. These results are similar to those observed in our study, thus confirming that HV stenosis is less frequent than HV thrombus.

In our study, HV thrombus was the most frequent HV abnormality and was observed in association with HV stenosis in 34.66% of patients. Our results are consistent with those of prior studies [10, 11]. One study found isolated HV thrombus in 71% of patients and HV thrombus in association with HV stenosis in the remaining 29% [10]. In another study, HV thrombus was observed in 90% of patients (Table 6) [11].

The results of our study revealed that a majority of patients had a chronic BCS from a clinical point of view and a majority of them had long-standing HV thrombus on imaging. Our results also confirm that diaphragmatic

Table 7. Literature data regarding number of obstructed HVs in patients with SBC

Authors [reference number]	1 HV *n* (%)	2 HVs *n* (%)	3 HVs *n* (%)
Chandrasekaran et al. [13]	15 (25.87)	11 (18.96)	32 (55.17)
Soyer et al. [15]	0 (0)	3 (13.64)	19 (86.36)
Kane et al. [14]	5 (45.45)	4 (36.36)	2 (18.18)
Current study	7 (3.98)	12 (6.82)	157 (89.21)

Table 6. Literature data regarding the nature of HV obstruction

Authors [reference number]	Imaging technique	Thrombosis *n* (%)	Stenosis *n* (%)	Thrombosis + stenosis *n* (%)
Boozari et al. [11]	US	29 (90.63)	0 (0)	3 (9.37)
Valla et al. [10]	*N. S.*	61 (70.74)	0 (0)	25 (29.06)
Mathieu et al. [17]	CT	*N. S.*	2 (5.26)	*N. S.*
Current study	US	115 (65.35)	7 (3.97)	54 (34.65)
	MDCT	122 (69.32)	6 (3.41)	48 (27.27)
	MRI	121 (68.75)	6 (3.41)	49 (27.84)

HV indicates hepatic vein. US indicates ultrasonography. CT indicates computed tomography. MDCT indicates multidetector-row computed tomography. MRI indicates magnetic resonance imaging. *N. S.* indicates not specified

stenosis of the IVC, which may correspond to fibrous or membranous transformation of a thrombus, is exceedingly rare. Finally, they revealed that obstruction of at least two HVs, whatever the clinical presentation, is the most frequent imaging finding. Similarly, obstruction of at least two HVs was predominant in the studies that have reported the number of affected HVs in BCS (Table 7) [13–15]. These data suggest that in patients with BCS, clinical symptoms related to portal hypertension and hepatocellular insufficiency occur after occlusion of at least two HVs. They also suggest that BCS is an insidious disease that remains clinically asymptomatic or is associated with non-specific symptoms for a long time in most patients.

Our study has several limitations. Of these, it must be acknowledged that a gold standard consisting of histopathological findings is lacking to definitely confirm the imaging findings. Another limitation is that imaging examinations were interpreted in consensus so that interobserver variability was not assessed.

In conclusion, the results of our study show that the chronic form is the most frequent imaging presentation of BCS. We also found that BCS is predominantly due to the obstruction of at least two HVs, either by long-standing thrombus or HV stenosis. Clinical data combined with the results of DCD-US, MDCT, and MRI using multiphasic acquisition support that BCS is a chronic and insidious disease, being more often expressed at an advanced stage. In addition, our results suggest that DCD-US should be the first line imaging modality for the diagnosis of BCS in patients with suggestive clinical symptoms. Our current results should warrant further evaluation of screening strategies in patients with risk factors for BCS to identify the disease at an early stage.

Acknowledgment. We thank Boualem Faraoun for excellent technical assistance and critical reading of the manuscript.

References

1. De Franchis R (2005) Evolving consensus in portal hypertension. Report of the Baveno IV consensus workshop on methodology of diagnosis and therapy in portal hypertension. J Hepatol 43:167–176
2. Janssen HL, Garcia-Pagan JC, Elias E, et al. (2003) European Group for the Study of Vascular Disorders of the Liver. Budd–Chiari syndrome: a review by an expert panel. J Hepatol 38:364–371
3. Valla D (2009) Primary Budd Chiari syndrome. J Hepatol 50:195–203
4. Valla D (2003) The diagnosis and management of the Budd–Chiari syndrome: consensus and controversies. Hepatology 38:793–803
5. Brancatelli G, Vilgrain V, Federle MP, et al. (2007) Budd–Chiari syndrome: spectrum of imaging findings. AJR Am J Roentgenol 188:W168–W176
6. Bayraktar UD, Seren S, Bayraktar Y (2007) Hepatic venous outflow obstruction: three similar syndromes. World J Gastroenterol 13:1912–1927
7. Ludwig J, Hashimoto E, McGill DB, van Heerden JA (1990) Classification of hepatic venous outflow obstruction: ambiguous terminology of the Budd–Chiari syndrome. Mayo Clin Proc 65:51–55
8. Dilawari JB, Bambery P, Chawla Y, et al. (1994) Hepatic outflow obstruction (Budd–Chiari syndrome): experience with 177 patients and a review of the literature. Medicine 73:21–36
9. Chawla Y, Kumar S, Dhiman RK, Suri S, Dilawari JB (1999) Duplex Doppler sonography in patients with Budd–Chiari syndrome. J Gastroenterol Hepatol 14:904–907
10. Valla D, Hadengue A, Younsi M, et al. (1997) Hepatic venous outflow block caused by short-length hepatic vein stenoses. Hepatology 25:814–819
11. Boozari B, Bahr MJ, Kubicka S, et al. (2008) Ultrasonography in patients with Budd–Chiari syndrome—diagnostic signs and prognostic implications. J Hepatol 49:572–580
12. Singh V, Sinha SK, Nain C, et al. (2000) Budd–Chiari syndrome: our experience of 71 patients. J Gastroenterol Hepatol 15:550–554
13. Chandrasekaran S, Cherian JV, Muthusamy AK, Joseph G, Venkataraman J (2007) Alternate pathways in hepatic venous outflow obstruction by color Doppler imaging. Ann Gastroenterol 20:218–222
14. Kane R, Eustace S (1995) Diagnosis of Budd–Chiari syndrome: comparison between sonography and MR angiography. Radiology 195:117–121
15. Soyer P, Rabenandrasana A, Barge J, et al. (1994) MRI of Budd–Chiari syndrome. Abdom Imaging 19:325–329
16. Kim TK, Chung JW, Han JK, et al. (1999) Hepatic changes in benign obstruction of the hepatic inferior vena cava: CT findings. AJR Am J Roentgenol 173:1235–1242
17. Mathieu D, Vasile N, Menu Y, et al. (1987) Budd chiari syndrome: dynamic CT. Radiology 165:409–413
18. Langlet P, Escolano S, Valla D, et al. (2003) Clinicopathological forms and prognostic index in Budd–Chiari syndrome. J Hepatol 39:496–501
19. Soyer P, Bluemke DA, Bliss DF, Woodhouse CE, Fishman EK (1994) Surgical segmental anatomy of the liver: demonstration with spiral CT during arterial portography and multiplanar reconstruction. AJR Am J Roentgenol 163:99–103
20. Darwish Murad S, Valla DC, de Groen PC, et al. (2004) Determinants of survival and the effect of portosystemic shunting in patients with Budd–Chiari syndrome. Hepatology 39:500–508
21. Bargalló X, Gilabert R, Nicolau C, et al. (2006) Sonography of Budd–Chiari syndrome. AJR Am J Roentgenol 187:W33–W41
22. Valla DC (2004) Hepatic venous outflow tract obstruction etiopathogenesis: Asia versus the West. J Gastroenterol Hepatol 19(Suppl 7):S204–S211
23. Wang ZG, Zhang FJ, Yi MQ, Qiang LX (2005) Evolution of management for Budd–Chiari syndrome: a team's view from 2564 patients. ANZ J Surg 75:55–63
24. Pisani-Ceretti A, Intra M, Prestipino F, et al. (1998) Surgical and radiologic treatment of primary Budd–Chiari syndrome. World J Surg 22:48–53
25. Camera L, Mainenti PP, Di Giacomo A, et al. (2006) Triphasic helical CT in Budd–Chiari syndrome: patterns of enhancement in acute, subacute and chronic disease. Clin Radiol 61:331–337